Received: 3 November 2023 | Accepted: 16 January 2024

DOI: 10.1002/jmv.29430

RESEARCH ARTICLE

JOURNAL OF MEDICAL VIROLOGY WILEY

Cross-reaction mediated by distinct key amino acid combinations in the complementary-determining region (CDR) of a monoclonal antibody

Chunyan Guo[1,2,3] | Qing Feng[1,2,3] | Xin Xie[1] | Yan Li[1,2,3] | Hanyu Hu[4] | Jun Hu[1,2] | Senbiao Fang[5] | Lijun Shang[6]

[1]Central Laboratory of Shaanxi Provincial People's Hospital, Xi'an, Shaanxi, China

[2]Research Center of Cell Immunological Engineering and Technology of Shaanxi Province, Xi'an, Shaanxi, China

[3]Shaanxi Provincial Key Laboratory of Infection and Immune Diseases, Xi'an, Shaanxi, China

[4]Shaanxi Ruiqi Biology Sci-Tech Co., Ltd., Xi'an, Shaanxi, China

[5]Department of Molecular Pharmacology, Tianjin Medical University Cancer Institute and Hospital, National Clinical Research Center for Cancer, Key Laboratory of Cancer Prevention and Therapy, Tianjin's Clinical Research Center for Cancer, Tianjin, China

[6]School of Human Sciences, London Metropolitan University, London, UK

Correspondence

Jun Hu, Central Laboratory of Shaanxi Provincial People's Hospital, Xi'an, Shaanxi, China.
Email: hjj6562@163.com

Senbiao Fang, Department of Molecular Pharmacology, Tianjin Medical University Cancer Institute and Hospital, National Clinical Research Center for Cancer, Key Laboratory of Cancer Prevention and Therapy, Tianjin's Clinical Research Center for Cancer, Tianjin, China.
Email: fangsenbiao@gmail.com

Lijun Shang, School of Human Sciences, London Metropolitan University, London, N7 8DB, UK.
Email: l.shang@londonmet.ac.uk

Funding information

Shaanxi Province Natural Science Basic Research Program, Grant/Award Number: 2023-JC-QN-0855; Key Research and Development Program of Shaanxi, Grant/Award Number: 2021ZDLSF01-03; Shaanxi Provincial People's Hospital, Grant/Award Number: 2021YJY-27

Abstract

In immunology, cross-reaction between antigens and antibodies are commonly observed. Prior research has shown that various monoclonal antibodies (mAbs) can recognize a broad spectrum of epitopes related to influenza viruses. However, existing theories on cross-reactions fall short in explaining the phenomena observed. This study explored the interaction characteristics of H1-74 mAb with three peptides: two natural peptides, LVLWGIHHP and LPFQNI, derived from the hemagglutinin (HA) antigen of the H1N1 influenza virus, and one synthetic peptide, WPFQNY. Our findings indicate that the complementarity-determining region (CDR) of H1-74 mAb comprised five antigen-binding sites, containing eight key amino acid residues from the light chain variable region and 16 from the heavy chain variable region. These critical residues formed distinct hydrophobic or hydrophilic clusters and functional groups within the binding sites, facilitating interaction with antigen epitopes through hydrogen bonding, salt bridge formation, and π–π stacking. The study revealed that the formation of the antibody molecule led to the creation of binding groups and small units in the CDR, allowing the antibody to attach to a variety of antigen epitopes through diverse combinations of these small units and functional groups. This unique ability of the antibody to bind with antigen epitopes provides a new molecular basis for explaining the phenomenon of antibody cross-reaction.

KEYWORDS

cross-reaction, epitope, immunodominant groups, key amino acid residues, molecular simulation

1 | INTRODUCTION

Antibodies are the culmination of the immune system's response to foreign antigens. They interact with antigens in a highly specific manner, recognizing antigenic determinants or epitopes, which include linear and conformational epitopes. These epitopes correspond to complementary determinants, known as paratopes, on the antibody.[1]

In 1936, Karl Landsteiner first observed that antigens and antibodies could cross-react, in addition to their specific reactions.[2] This phenomenon suggests that, beyond their specific antigenic epitopes, many antigens share common antigen epitopes, termed co-antigens. Typically, cross-reaction occurs due to linear epitopes with identical sequences or conformational epitopes with similar structure.[3] For nearly a century, numerous pathogens and their products have been reported to cross-react with human tissues, potentially inducing autoimmune diseases. This cross-reactivity involves common epitopes between autoantigens in autoimmune diseases and natural microbial proteins; these are either linear epitopes with the same sequence or conformational epitopes with the same or similar structure.[4] These include the PPPGRRP peptide of Epstein–Barr virus nuclear antigen-1 and the spliceosome SmB/B′ peptide in systemic lupus erythematosus patients,[5] along with epitopes found in colon tissue and *Escherichia coli* O14.[6] Further, the overlapping sequence between the M5 protein (85–103) region of *Streptococcus* and cardiac myosin results in the cross-reactivity between streptococcus M5 protein and cardiac histonein.[7]

However, cross-reactivity can also occur in the absence of confirmed co-antigens in certain autoimmune disorders. For example, antibodies produced to human T-lympho virus type 1 (HTLV-1) infection can interact with hnRNPA1, leading to myelopathy/tropical spastic paraplegia. Levin's use of the mimotope multipin peptide system identified the dominant epitope KHFRETEV in HTLV-1, which does not correspond to any similar sequence or conformational epitopes on hnRNPA1.[8] Similarly, monoclonal antibodies (mAbs) of H1N1 influenza virus hemagglutinin (HA) have been found to interact with islet cell prohibition proteins without any homologous sequence or conformational epitopes with similar structures between HA and prohibition proteins.[9] In most cases, there is no homologous sequence or conformational epitopes with similar structure between autoantigens and microbial antigens, and this phenomenon remains unexplained. Consequently, direct evidence linking pathogenic microbial infection and autoimmune disease is limited, impacting early disease diagnosis and treatment.

A previous study focusing on the localization of anti-2009 H1N1 influenza virus mAb binding to a target antigen,[10] yielded three mAbs that recognized two distinct sequences on HA antigens. Influenza viruses are categorized into four types: A, B, C, and D, with type A being the most severe. The 1918 influenza A (H1N1) outbreak in Spain and the 2009 H1N1 outbreak in Mexico had significant societal impacts.[11] This study concentrated on the H1-74 mAb produced by the 2009 H1N1 influenza virus HA protein, which reacts with two peptides, LVLWGIHHP (191aa–199aa) and LPFQNI (307aa–312aa), derived from the HA protein. We aimed to investigate the molecular mechanism of antibody cross-reaction and determine if varying combinations of key amino acid residues within the complementary determining region (CDR) of antibody molecules could facilitate cross-reaction. This study also sought to clarify the link between pathogenic microbial infection and autoimmune disease, even in the absence of homologous sequences or similar conformational epitopes in cross-reacting molecules. Early removal of pathogenic microorganisms in patients to prevent the production of such cross-reactive antibodies may offer a new approach to treating autoimmune diseases.

The essential residues from antigens forming epitopes are termed "immunodominant groups." The key amino acids in the variable region of an antibody that interact with these immunodominant groups are referred to as "key amino acid residues," for distinction.

2 | MATERIALS AND METHODS

Detailed descriptions of the experiments are provided in Supporting Information S1: Sections S1 and S2.

2.1 | Methods

2.2 | Distribution of polypeptides LP-9 and LI-6 on the HA crystal structure

The HA crystal structure of the influenza A (H1N1) virus was obtained from the PDB database. The 3LZG protein sequence was referenced to locate the distribution regions of LP-9 and LI-6 on the HA crystal using PyMOL software.

2.3 | Cloning, sequencing, and molecular modeling of H1-74 mAb's light and heavy chain variable regions

Following established procedures, messenger RNA was extracted from H1-74 mAb hybridoma cells[12] and converted into complementary DNA for gene cloning. The variable regions of the light and heavy chains of H1-74 mAb were cloned, sequenced, and molecularly modeled (Supporting Information S1: Sections S2.1 and S2.2).

2.4 | Identification (LXXXI) of amino acid substitutions for LVLWGIHHP skeleton in 6-peptide LPFQNI that maintain H1-74 mAb binding through molecular simulation

Using MOE software, we analyzed the dominant conformational structures of the LI-6 peptide chain. Antibody-antigen docking

provided a reliable model of their interactions. Docking was performed using Amber10, and the most effective antigen-antibody binding mode was selected for analyzing amino acid mutations in 6-peptide LPFQNI. Virtual mutation methods were employed to identify mutants in LI-6 that affected binding activity with H1-74 mAb (Supporting Information S1: Sections S2.3 and S2.4).

2.5 | Analysis of the binding activity of mutant polypeptides

Enzyme-linked immunosorbent assay (ELISA) plates were coated with H1N1 influenza virus HA antigen at a concentration of 2 μg/mL. Peptides LP-9, LI-6, the enhanced mutant peptide WY-6, and the attenuated mutant peptide LPGQGI were incubated with H1-74 mAb at 37°C for 1 h. The mixture was added to the HA-coated ELISA plates. The assay was conducted using standard ELISA procedures (100 μL per well, 37°C for 1 h). The mixture was washed and then sheep anti-mouse enzyme-labeled antibody was added to it. The other steps were the same as in conventional ELISA. Using TMB color rendering, the $OD_{450\ nm}$ value of each well was determined. The inhibition rate was calculated according to the $OD_{450\ nm}$ value of each well[12,13]: inhibition rate = (untreated control group − experimental group)/untreated control group. An inhibition rate ≤0.4 indicated nonrecognition of the epitope by the antibody. Rates 0.4 and 0.8 suggested partial recognition and ≥0.8 indicated full recognition.

2.6 | Characterization of H1-74 binding to LP-9, LI-6, and WY-6

Three-dimensional structural models of LP-9, LI-6, and WY-6 were constructed using UCSF Chimera software. Initial molecular dynamics simulations were performed to determine the rational structural conformations of three polypeptides. Flexible molecular docking of H1-74 mAb with these peptides was then executed using Rosetta software. Both proteins and peptides were set as flexible for 100 docking conformations. The conformation with the lowest docking energy for each peptide (LP-9, LI-6, and WY-6)-H1-74 pairing was selected for further molecular dynamics simulation using Amber16 (Supporting Information S1: Section S2.5).

2.7 | Preparation and characterization of monoclonal and polyclonal antibodies using LP-9, LI-6, and WY-6 as immunogens

Consistent with prior research, peptides were conjugated to bovine serum albumin (BSA) and keyhole limpet hemocyanin (KLH) carrier proteins[14,15] using 1-(3-dimethylaminopropyl)-3-ethylcarbodiimide (EDC) activators for immunization. We used EDC to activate the carboxyl terminals of three polypeptides, coupled with the carrier proteins BSA and KLH.[16] The cross-linking of the polypeptides to the carriers was outsourced to Shanghai Qiangyao Biological Company. The preparation and characterization of both monoclonal and polyclonal antibodies are described in Supporting Information S1: Sections S2.6–S2.10.

3 | RESULTS

3.1 | Amino acid sequences of light and heavy chain variable regions of H1-74 mAb and their structural characteristics

Previous studies identified two peptides bound by H1-74 mAb at positions 191-LVLWGIHP-199 (LP-9) and 307-LPFQNI-312(LI-6) on the HA antigen, respectively.[10] The HA molecule naturally split into HA1 and HA2, containing 319–328 amino acids and 221–222 amino acids, respectively. Thus, LP-9 and LI-6 were located in HA1 (Figure 1A).

We extracted the amino acid sequences of the variable regions of H1-74 mAb's light and heavy chains. Analysis using abYsis software (http://www.abysis.org/abysis/) indicated distinct structural features in the skeletal (FR) and variable (CDR) regions of the light and heavy chains of H1-74 (Figure 1B). Sequence analysis against the RCSB PBD database, followed by homology modeling for H1-74 mAb using Modeller software, selected crystal structures (PDB ID: 5twp and 5nj6) with sequence identities of 84.35% and 92.45% to H1-74 VH and VL regions, respectively, as modeling templates. We focused primarily on five binding regions (Figure 1C). Binding region 1C-A comprised amino acid residues of N36, T58, N57, Y37, and Y105 in both H1-74 VL and H1-74 VH. N57 and T58 were identified as polar hydrophilic amino acid residues, forming hydrogen bonds with polypeptide groups. Y37, Y105, and N36 possessed side chains that could form hydrophobic binding regions. Binding region 1C-B's Amide-$C(O)NH_2$ group atop N40's side chain could form hydrogen bonds with polypeptides below, while W55, L104, and M110 could establish a hydrophobic binding pool. In binding zone 1C-C, residues F220, Y214, M110, and W52 formed a deeper binding pocket with a higher degree of hydrophobicity. H212, located at the pocket's base, established polar rivet interactions with neighboring amino acid residues on the polypeptide bounding region. Binding region 1C-D, compact and small at the protein's top, contained highly polar R218 and D67 amino acid residues, capable of forming a strong salt bridge with associated peptides. A66, W52, F220, T64, and Y65 created shallow hydrophobic binding pockets. Binding region 1C–E consisted of multiple amino acids with distinct characteristics, including polar amino acid residues such as R216, H212, and S217, and hydrophobic amino acid residues such as Y214 and Y155. The polar amino acid residues could establish a salt bridge with strong negatively

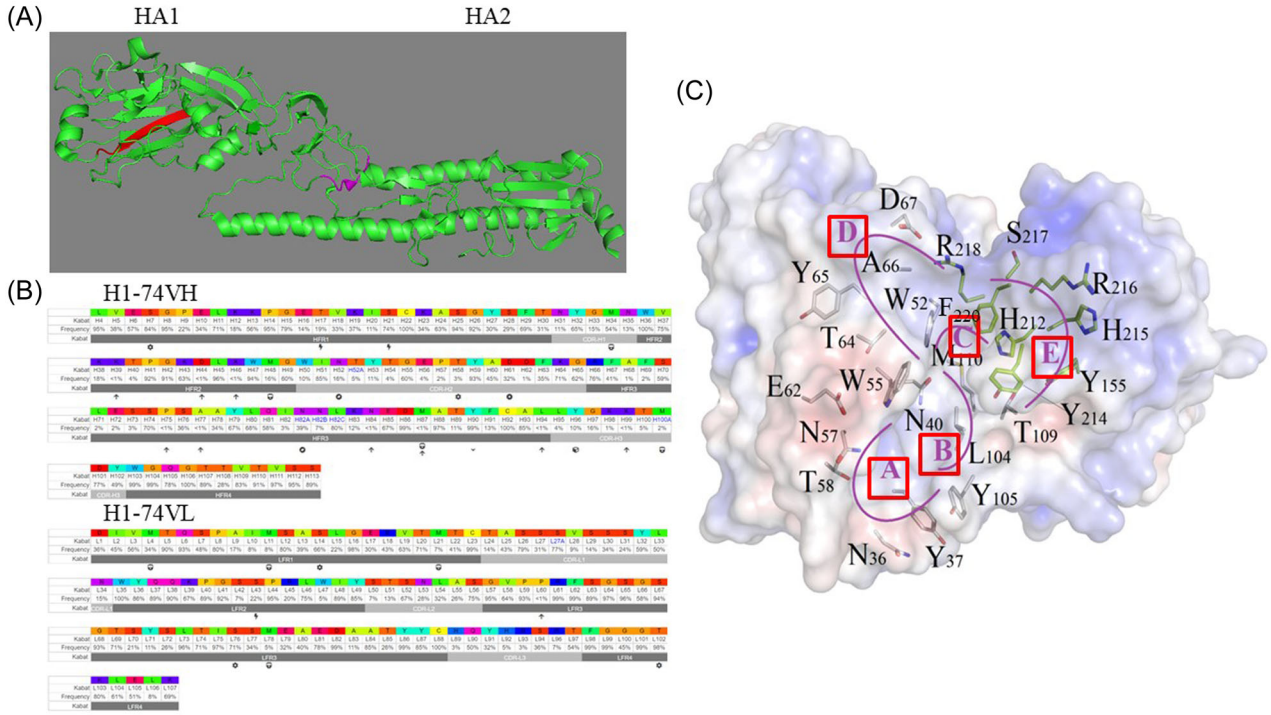

FIGURE 1 Simulation structure of H1-74 mAb variable region formation of hydrophobic, hydrophilic pockets which may form salt bonds, hydrogen bonds, and so on. (A) The positions of LP-9 and LI-6 on the three-dimensional structure of hemagglutinin (HA). Red represented LP-9 and purple represented LI-6. (B) The variable region gene of light and heavy chain of H1-74 mAb was cloned and sequenced. (C) The H1-74 mAb consisted of light and heavy chains. One long antigen-binding pocket was formed by 8 and 16 amino acids from the H1-74 VL and H1-74 VH subunit, respectively. To ensure one more intuitive view of binding sites, five polypeptide-binding regions of binding pocket on the H1-74 protein (region A–E) were divided based on the geometric shapes and physicochemical properties.

charged amino acids in polypeptides, while hydrophobic ones enabled an aromatic stacking effect by forming π–π stacking with identical amino acid residues in polypeptides through their benzene rings.

3.2 | Virtual mutation screening of polypeptide LI-6

When the peptides LPFQNI and LVLWGIHHP are combined with H1-74 they contain the same "LXXXXI" structure; this suggests a conformational epitope. To investigate mAb binding to antigenic epitope peptides with completely different structures, we mutated LPFQNI's residues into 20 different amino acid residues using Pymol software, then assessed each mutation's affinity to H1-74 via molecular docking. L307-W and I 312-Y mutations improved binding affinity and structural stability (Table 1). F309-G and N311-G mutations in LPGQGI weakened affinity to H1-74. This indicated that the mAb can bind to two antigen peptides (WPFQNY and LVLWGIHHP) with completely different structures. Finally, we obtained an artificially modified six peptide WPFQNY that can still bind to H1-74 and was completely different from the LVLWGIHHP sequence and structure, and an artificially modified six peptide LPGQGI with significantly weakened binding activity to H1-74.

3.3 | Changes in the binding characteristics of polypeptides to H1-74 mAb, pre- and postmodifications

Analysis showed LPFQNI and WPFQNY occupying six identical binding positions in H1-74's protein binding groove (Figure 2A).

At binding position 1 (Figure 2B), HI-74's antibody protein was surrounded by amino acids Y65, K70, and D67, wherein the hydrophobic carbon chain hydrophobic groups on the Y65 benzene ring, K70, and D67 formed a planar hydrophobic binding region. When bound to a polypeptide, the amino acid L side chain group on the polypeptide LPFQNI was small and the hydrophobic effect was weak. The W amino acid side chain indole group was larger and formed a stronger hydrophobic binding surface than L with the surrounding amino acids, especially the side chain phenol group on the Y65 amino acid, which was more conducive to the combination of both sides.

In the binding position 2 (Figure 2C), the amino acids bound on both polypeptides were P, and the volume of the side chain pentacion C-N heterocyclic was unchanged, so the change was less pronounced.

The position 3 region (Figure 2D) consisted of residues R218, W52, F220, H212, and Y105. Compared to F in LPFQNI, the side chain phenyl ring group of residue F on WPFQNY could be inserted

TABLE 1 The binding activity of different amino acid mutants of LPFQNI polypeptide with H1-74 mAb.

	Mol	Mseq	Sseq	Museq	Mutation	Affinity	dAffinity	Stability	dStability
1	FvModel_fv_mode	1	4	3	3: I312Y	−59.4312	−4.8124	−717.4512	1.0161
2	FvModel_fv_mode	1	5	4	3: L307W	−60.5072	−4.8984	−715.3697	1.3196
3	FvModel_fv_mode	1	4	17	3: I312F	−58.8166	−4.1979	−717.8752	0.5921
4	FvModel_fv_mode	1	4	4	3: I312R	−57.4777	−2.8589	−718.0372	0.4301
5	FvModel_fv_mode	1	4	14	3: I312R	−57.4303	−2.8115	−718.0150	0.4523
6	FvModel_fv_mode	1	5	11	3: L307G	−58.3651	−2.3473	−714.9127	1.7766
7	FvModel_fv_mode	1	5	3	3: L312G	−58.3651	−2.3473	−714.9126	1.7767
98	FvModel_fv_mode	1	3	6	3: N311E	−56.3202	2.1514	−710.1723	1.2134
99	FvModel_fv_mode	1	5	9	3: L307I	−53.8634	2.1514	−715.6546	1.0347
100	FvModel_fv_mode	1	4	5	3: I312G	−51.9063	2.7124	−715.8117	2.6556
101	FvModel_fv_mode	1	6	15	3: F309A	−51.7348	2.8484	−716.6816	0.7116
102	FvModel_fv_mode	1	3	3	3: N311S	−54.9134	3.5583	−710.5451	0.8406
103	FvModel_fv_mode	1	3	12	3: N311S	−54.9075	3.5641	−710.5446	0.8390
104	FvModel_fv_mode	1	6	4	3: F309G	−49.4636	5.1196	−715.9417	1.4514
105	FvModel_fv_mode	1	3	4	3: N311G	−52.1555	6.3162	−710.0386	1.3471

Note: If "dAffinity" was negative, it meant that the affinity of the mutant became stronger, if "dAffinity" was positive, it meant that the affinity of the mutant became weaker.

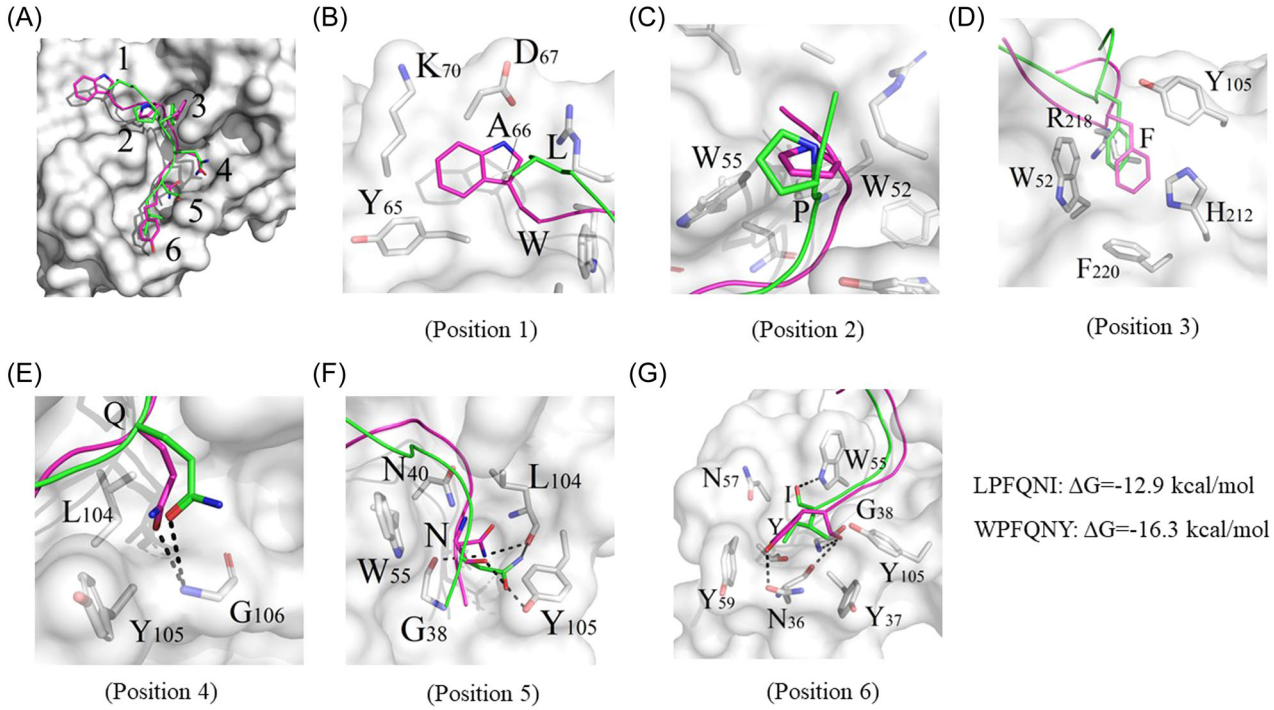

FIGURE 2 Variable region structure docking analysis of LPFQNI, WPFQNY, and H1-74. Binding modes of peptides LPFQNI (colored green) and WPFQNY (colored magenta) to the protein H1-74. The binding surface was shown as white surface. Residues forming the binding interface within 4.5 Å from each other between peptides and H1-74 were shown as sticks. Hydrogen bonds were shown as black dashes. (A) The peptides LPFQNI and WPFQNY occupied the identical six binding positions in the H1-74 protein binding groove. (B–G) Binding modes difference of peptides LPFQNI and WPFQNY to the H1-74 at six binding positions 1–6.

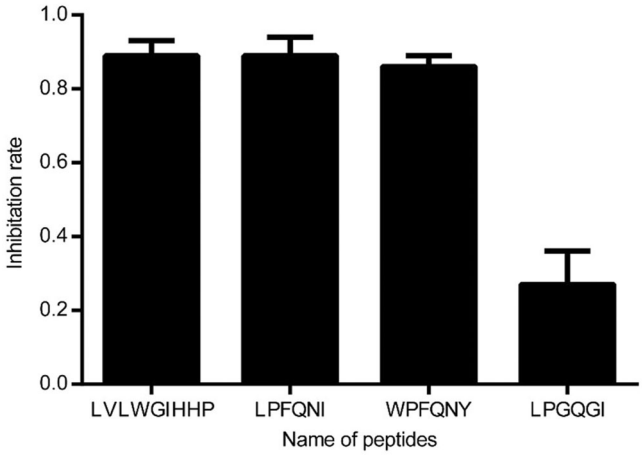

FIGURE 3 Inhibition rate of the reaction of original and mutant peptides with H1-74.

deeper into the hydrophobic binding pocket. A better hydrophobic matching effect was formed between the indole hydrophobic planar group on the W52 amino acid and the benzene ring on the Y105. In addition to the hydrophobic effect, amino acid F on WPFQNY also formed a new hydrophobic interaction with the amino acid F220 side chain benzene ring deep in the pocket, so that the WPFQNY polypeptide bound to H-74, and the hydrophobic effect in the position 2 region was stronger than LPFQNI.

In the position 4 region (Figure 2E), the amino acids on both polypeptides were Q, and the binding patterns were not much different.

In the position 5 region (Figure 2F), the N amino acid terminal N atom on LPFQNI only formed a hydrogen bond with the O atom on L104, while the N terminal N atom on WPFQNY formed multiple hydrogen bonds with the oxygen atom on G38, the skeleton oxygen atom on L104, and the phenol group at the end of the Y105 side chain. Therefore, WPFQNY formed a stronger polar binding effect than LPFQNI in the position 5 region.

Within position 6 (Figure 2G), I only formed a hydrogen bond with W55. Y formed hydrogen bonding with N36, Y37, and G38. Although the hydrogen bonding system was comparable, Y formed a stronger hydrophobic interaction with Y37 and Y59. Overall, when the polypeptide LPFQNI was transformed into a polypeptide WPFQNY, the binding activity of the latter to H1-74 was enhanced.

3.4 | Binding activity of polypeptides to H1-74 mAb

The binding of H1-74 to the H1N1 antigen of the influenza virus was assessed by performing blocking experiments using polypeptide LP-9, LI-6, WY-6, and LPGQGI. The binding activity between H1-74 mAb and four polypeptides was tested and verified. Based on the inhibition rate ≤ 0.4 indicated that the antibody did not recognize the epitope. The inhibition index between 0.4 and 0.8 indicated that the epitope recognized by the antibody was related to it. The inhibition rate ≥ 0.8 indicated that the antibody recognized the epitope. it was concluded that the inhibition rates of LP-9, LI-6, and WY-6 on the binding of H1-74 and HA were all above 0.8, indicating that these three peptides were recognized by H1-74. Even after the substitution of LXXXI with WXXXY in LPFQNI, it was found that WPFQNY still possessed good binding affinity to H1-74, despite having a completely different sequence from that of LVLWGIHHP (Figure 3).

3.5 | Interaction patterns of polypeptides with H1-74

To check the stability of three different systems, RMSD values were tested to monitor the conformation fluctuations of complexes over 100 ns molecular dynamics simulations (as shown in Supporting Information S1: Figure S1), all systems had reached equilibrium. Average structure for each system was extracted from the equilibrated trajectories. To investigate the molecular basis for the cross-reaction between antibody and antigen epitope peptide binding, interaction patterns of polypeptide LP-9, LI-6, and WY-6 with the H1-74 mAb were analyzed to understand how a mAb binds to different epitopes of different antigens (Figure 4).

When LVLWGIHHP was bound to H1-74 mAb, compared with the two polypeptides LI-6 and WY-6, it could be spread more in the H1-74 antibody binding cavity, so the binding energy was the lowest (Figure 4A). L, V, and L adhered to the protein surface shallow, hydrophobic pockets, and the surrounding amino acids were expected to form a good hydrophobic interaction. This binding region consisted of amino acids W52, W55, K70, and D67, where indole groups on the W52 and W55 amino acids formed a hydrophobic matching effect. W: The indole group of its side chain was particularly large, and it was inserted deeply into the hydrophobic pocket area of the antibody, which formed an excellent hydrophobic matching effect with the hydrophobic binding pocket composed of amino acids such as W52, W55, M110, T109, Y214, N40, and so on. In particular, an aromatic stacking effect was formed with the Y214 benzene ring and the W52 indole group. G and I: The former skeleton C(=O)–N and the lateral side chain carbon chain, between the surrounding amino acids, especially W55 and Y37, formed a good hydrophobic compensation effect. H and H: amino acids formed neutral polar interactions with nearby amino acids, qualitatively reflected in hydrogen bonding systems. These hydrogen bonds included histidine H–N (nitrogen)…O (oxygen)–Y105 and histidine H–N (nitrogen)…O (oxygen)–N36. P: The oxygen atoms of the terminal skeleton formed a good hydrogen bond with the N atoms on N57, and the hydrophobic interaction between the carbon and nitrogen pentaary rang on the side chain and the surrounding amino acids was formed.

In the LPFQNI system (Figure 4B), L and P could adhere to the shallow surface of the protein, hydrophobic pockets, forming a good hydrophobic interaction. The amino acids R218, D67, K70, A66, T64,

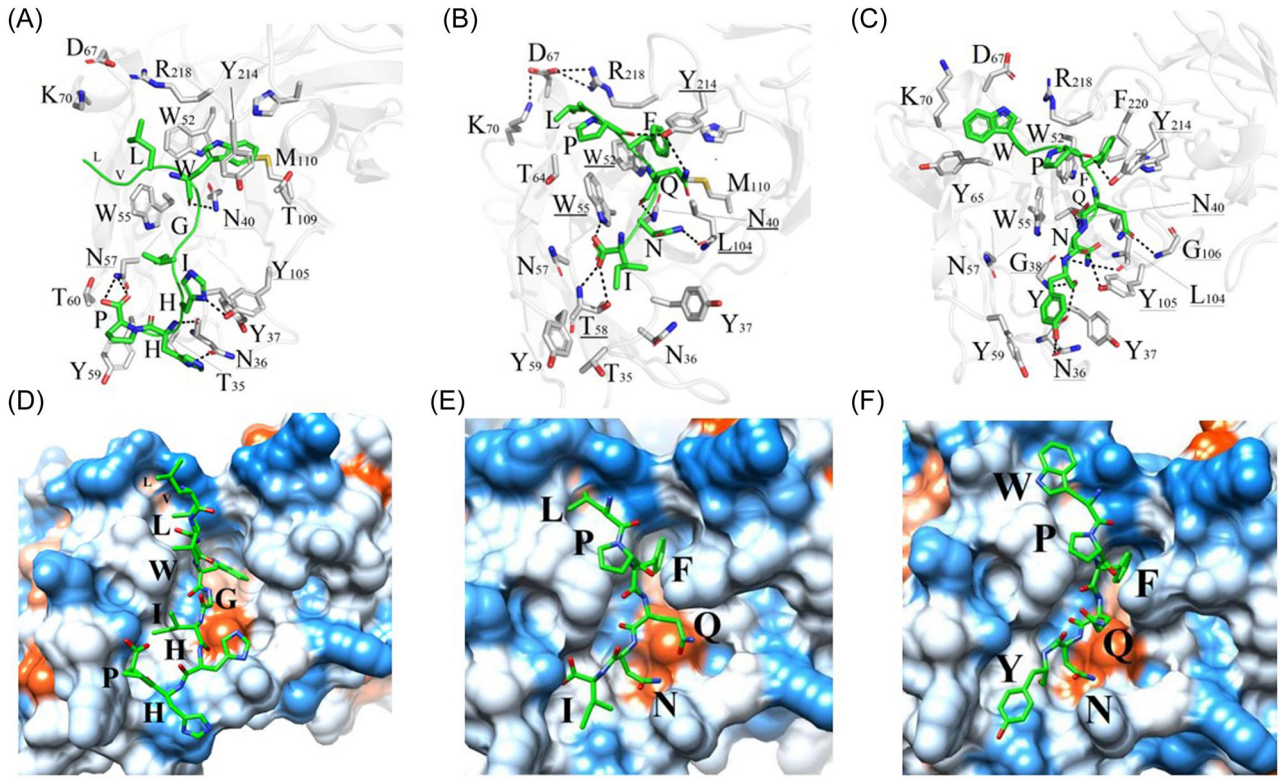

FIGURE 4 Binding pattern of H1-74 mAb with polypeptide LP-9, LI-6, and WY-6. (A–C) Schematic of binding interface between peptides and H1-74 mAb. Binding interface regions for peptides and H1-74 mAb were colored as follows: H1-74 in white and peptides in green. Key residues forming binding interface were shown as sticks and colored as white and green. The hydrogen bonds were shown in dotted lines. (D–F) Hydrophpbic and hydrophilic binding surfaces for H1-74 and peptides complexes.

Y214, and W52 and polypeptides, especially between P and I, formed an excellent hydrophobic matching effect on the H1-74 protein. In addition, the oxygen atoms in the proline P backbone could form hydrogen bound with phenol on Y214. F: The sidechain phenyl cyclic group was a hydrophobic chemical group, which was inserted into the hydrophobic binding pocket composed of amino acids such as W52 and Y214 on the insertion protein, forming a strong hydrophobic interaction pattern. Q and N: The skeleton C(=O)–N formed a good hydrophilic compensation effected with the surrounding amino acids, including glutamine Q–N (nitrogen)…O(oxygen)-Y214, glutamine Q–O(oxygen)…N (nitrogen)-N40 and asparagine N–N(nitrogen)…O (oxygen)-L104. I: C atoms on amino acid side chain groups formed a good hydrophobic interaction with the surrounding hydrophobic environment.

In the WPFQNY system (Figure 4C), W and P were surrounded by hydrophobic pockets formed by Y65, K70, D67, and R218, forming a good hydrophobic effect. Compared with L in LPFQNI, the tryptophan W side chain group was larger, so the hydrophobic effect of the side chain group was stronger. P: In addition to the hydrophobic interaction, hydrogen bonding with Y214 was also formed. F had good PI–PI interaction with W52 and good hydrophobic interaction with the benzene ring side chain on Y214. Compared with the F in LPFQNI, the amino acid F in WPFQNY was inserted deeper into the pocket, in addition to the hydrophobic effect described above, a new hydrophobic interaction with the amino acid F220 was formed deep in the pocket, so this part had a stronger effect. Q exhibited hydrogen bonding with N40 and G106. N exhibited hydrogen bonding with G38, L104, and Y105, of which G38 and Y105 were new hydrogen bonding systems. Y exhibited hydrogen bonding with N36, G38, and Y37. Although the hydrogen bonding system was comparable to amino acid I in the polypeptide LPFQNI, it formed a stronger hydrophobic interaction with Y37 and Y59.

It was discovered that upon binding of the H1-74 to various polypeptides, the two molecules mutually induced and conformed to each other, resulting in an optimal geometric and energetic match. The binding energy between the polypeptides LP-9, LI-6, and WY-6 and H1-74 were −21.9, −12.9, and −16.3 kcal/mol, respectively, indicating that despite having completely different sequences, the two short peptides had a strong binding affinity for H1-74 (Table 2).

3.6 | Antipeptide serum production in peptide-immune mice

To prepare antipolypeptide serum, BALB/c mice (6–8 weeks) were immunized with LP-9, LI-6, and WY-6. The resulting serum was then tested for antibodies against H1N1 influenza virus to determine whether the polypeptides contained antigen epitopes of the influenza virus HA antigen, which could bind to H1-74 (Table 3).

TABLE 2 The bond energy of H1-74 mAb binding to each immunodominant group on peptide LP-9, LI-6, and WY-6.

	H1-74			H1-74			H1-74	
Immunodominant group of peptide	A combination of key amino acid residues	Bond energy	Immunodominant group of peptide	A combination of key amino acid residues	Bond energy	Immunodominant group of peptide	A combination of key amino acid residues	Bond energy
L	*K70*, D67, W55, W52	−2.2	L	R218, D67, *K70* A66	−1.3	W	R218, D67, *K70*, A66, Y65	−2.6
V	W52, W55	−2.7	P	T64, Y214	−1.9	P	Y65, W52, Y214	−1.8
L	W52, W55, R218	−2.4	F	W52, Y214	−3.8	F	W52, Y214, F220	−4.0
W	W52, W55, M110, *T109*, Y214, N40	−4.5	Q	N40, M110, W52	−2.0	Q	Y214, N40, M110, W52, W55	−2.6
G	N40, Y214, W55	−1.3	N	L104	−1.5	N	*G38*, L104, Y105, *G106*	−2.3
I	N57, W55, Y37	−2.3	I	W55, T5,	−2.4	Y	*G38*, N36, Y37, *Y59*, W55	−3.0
H	Y105, Y37, N36	−3.8						
H	N36, *T35*	−1.8						
P	*Y59*, N57, *T60*	−0.9						
Total bond energy	ΔG = −21.9 kcal/mol		ΔG = −12.9 kcal/mol			ΔG = −16.3 kcal/mol		

TABLE 3 Reaction characteristics of polyclonal antibodies against polypeptides LP-9, LI-6, and WY-6.

Coated antigens	Mice			
	No1	**No2**	**No3**	**No4**
WY-6-KLH	10^5	10^5	10^5	10^5
H1N1	No	No	No	No
	No1	**No2**	**No3**	**No4**
LI-6-KLH	10^5	10^5	10^5	10^5
H1N1	10^3	10^3	10^3	No
	No1	**No2**	**No3**	**No4**
LP-9-KLH	10^5	10^5	10^5	10^5
H1N1	10^3	10^4	No	10^4

Note: The data in the table showed antibody titers. The serum of immunized mice was continuously diluted 10-fold starting from 1:1000. "No" meant that the mouse immune serum did not respond when diluted 1000 times.

TABLE 4 Identification of reaction characteristics of anti-LP-9 mAbs with three polypeptides and influenza virus antigens.

Coated antigens	LP-9-1	LP-9-3	LP-9-4	LP-9-5	LP-9-6	LP-9-7	LP-9-9
LP-9-KLH	20.14 ± 0.08	20.37 ± 0.07	20.25 ± 0.07	19.93 ± 0.10	18.78 ± 0.09	17.97 ± 0.10	13.48 ± 0.14
LI-6-KLH	22.54 ± 0.07	25.68 ± 0.10	24.98 ± 0.13	25.86 ± 0.12	3.22 ± 0.05	18.25 ± 0.07	19.72 ± 0.12
WY-6-KLH	20.53 ± 0.12	23.01 ± 0.12	25.30 ± 0.18	23.64 ± 0.10	3.61 ± 0.04	19.30 ± 0.10	18.52 ± 0.08
H1N1	0.94 ± 0.04	0.77 ± 0.03	0.69 ± 0.04	0.43 ± 0.03	10.12 ± 0.02	0.60 ± 0.04	0.64 ± 0.04
A3	0.77 ± 0.04	0.99 ± 0.04	1.07 ± 0.02	0.84 ± 0.04	4.72 ± 0.04	0.98 ± 0.04	1.27 ± 0.06
308	0.68 ± 0.03	0.88 ± 0.04	0.88 ± 0.02	0.75 ± 0.03	0.85 ± 0.02	0.84 ± 0.02	0.85 ± 0.02
PR8	0.96 ± 0.04	1.02 ± 0.04	0.87 ± 0.04	0.47 ± 0.03	1.04 ± 0.04	0.86 ± 0.04	0.63 ± 0.03
501	0.77 ± 0.02	0.92 ± 0.03	0.87 ± 0.03	0.55 ± 0.03	1.11 ± 0.03	0.82 ± 0.03	0.87 ± 0.01
H7N2	0.90 ± 0.03	0.92 ± 0.04	1.20 ± 0.06	0.56 ± 0.03	0.52 ± 0.03	1.03 ± 0.04	1.15 ± 0.03

Note: The values in the table were the ratio of the optical density (OD) value detected by enzyme-linked immunosorbent assay in the experimental group to the OD value in the SP2/0 control group (the antibody and SP2/0 negative control used cell culture supernatant, and the negative control OD value was less than 0.05, it was calculated as 0.05), and the P/N ≥ 2.5 result was positive. $n = 3$.

The results showed that both the LP-9 and LI-6 from the influenza virus HA antigen retained the antigen epitopes from the influenza virus HA antigen thereby inducing the production of antibodies against the H1N1 influenza virus HA antigen. However, WY-6, which was a modified version of LI-6, was incapable of stimulating the body to produce antibodies against H1N1 influenza virus HA antigens. This implied that WY-6 was not an antigen on the H1N1 influenza virus; H1-74 mAb produced by the influenza virus was able to bind to antigenic epitopes from different sources. This result indicated that mAbs had an ability for binding to many different epitopes of different antigens.

3.7 | Analysis of reaction characteristics of mAbs prepared from three polypeptides

Following immunization with three polypeptides, mAbs were screened and their reaction characteristics were examined to ascertain whether the epitopes bound by H1-74 were identical across all three polypeptides.

The analysis of their reaction characteristics showed that at least one of the mAbs from each natural polypeptide could interact with the antigen of the H1N1 influenza virus (Table 4 and Supporting Information S1: Table S2), suggesting the presence of influenza virus H1N1 antigen epitope on LP-9 and LI-6. Nevertheless, none of the 20 mAbs targeting artificially altered polypeptide WY-6 exhibited reactivity towards H1N1 (refer to Supporting Information S1: Table S3), thereby providing additional evidence that the epitope formed by H1-74 on WY-6 and the influenza virus HA antigen were dissimilar. Further analysis of the immunodominant groups of mAbs binding polypeptides LP-9, LI-6, and WY-6 showed that, for example, polypeptide LI-6 produced at least seven different immunodominant group combinations (Supporting Information S1: Table S4). This provides a foundation for analyzing the mechanism of antibody cross-reaction from the level of epitope composition.

4 | DISCUSSION

Antibody cross-reaction with antigen binding is a widely observed phenomenon in immunological research. Significant strides have been made in understanding both the specific responses to antigens and antibodies, and the cross-reactivity where antibodies bind to different antigens. Current knowledge suggests that cross-reaction is often due to identical linear epitopes or similar conformational/discontinuous epitopes on different target antigens.[17,18]

In bioinformatics studies of cross-reactivity epitopes, a common starting point is the search for sequence similarity. BLAST, a tool from NCBI, has been utilized to identify potential cross-reactivity epitopes in COVID-19 protein.[19] This approach was initially used to explore the possibility that antigen epitope similarity might contribute to the neurological symptoms of COVID-19 and the pathogenesis of autoimmune diseases after COVID-19 infection.[20–22] However, subsequent research revealed limitations to this approach; sequence similarity alone is insufficient for reliably predicting cross-reactivity epitopes between proteins. For instance, Yuan's study on a neutralizing monoclonal antibody (CR3022) demonstrated its cross-reaction with the S protein of both COVID-19 and SARS. The crystal structure of CR3022 and RBD complex of two proteins was analyzed by X-ray crystal diffraction. The analysis revealed significant differences in the conformational epitopes between the COVID-19 and SARS proteins. Different binding modes between CR3022 and different epitopes on the two proteins by chemical bonds could also cross-react. This suggested that antibodies can cross-react with multiple epitopes, even those with different linear sequences or conformational structures.[23] In our study, we focused on the H1-74 mAb, targeting the influenza virus HA antigen, and its binding to two specific antigenic epitope peptides, 191-LVLWGIHHP-199 and 307-LPFQNI-312.[10] We combined bioinformatics analysis with the classical ELISA method to investigate the mechanism of antibody cross-reaction.[24,25]

In our comparison of the peptides 191-LVLWGIHHP-199 and 307-LPFQNI-312, we identified a common "LXXXXI" structure (Figure 1A), suggesting they might represent similar conformational epitopes. To explore if H1-74 mAb could bind to two distinct short peptides with different conformations, we created a new structure to replace the "LXXXXI" structure in LI-6. We performed virtual saturation mutations on LI-6 using computer molecular simulation, leading to the discovery of an affinity-enhanced mutant WY-6. This mutant's binding to H1-74 was confirmed by biological experiments (Figures 2 and 3). The ability of H1-74 to bind to two antigenic epitope peptides with completely different sequences or conformations indicates that the mAb exhibited cross-reactivity. This finding helps explain why antibodies against pathogens can bind to human tissues without similar or identical sequences or conformations.[8]

Recent research has delved into the cross-reaction mechanism between antibodies and antigen epitopes. It was found that antibodies could induce conformational changes in target antigen epitopes, leading to allosteric transformations that make them compatible for binding.[26] This implies that the geometric arrangement within some epitopes imparts cross-reactive capabilities to antibodies.[27] Moreover, crystal structure analysis has shown that a single antibody can exhibit multiple specificities by binding to various antigens at different CDR regions, due to variations in ligand placement.[28,29] Based on 3D structural analysis, only a small portion (20%–33%) of amino acid residues in the CDR of the antibodies were responsible for antigen binding, and this section of the amino acid residues was highly variable in each antibody molecule. A single antibody's CDR can have multiple binding recognizing different epitopes.[30,31] This conformational diversity of sequences, while enhancing the antibody library's effectiveness, can also lead to autoimmunity and allergies.[32]

We refined our approach by excluding identical linear epitopes or similar conformational epitopes, focusing instead on the dominant foundation for analyzing the interaction patterns of H1-74 mAb with three epitope peptides LP-9, LI-6, and WY-6 through molecular simulation. Our findings highlight the complexity in mAb formation, involving hydrophobic and hydrophilic units, and groups capable of forming hydrogen bonds, salt bonds, and π–π stacking (Figure 4). We pinpointed the locations of these structures. The interaction process begins with collisions between groups on the antibody and antigen epitope, leading to molecular binding as the sum of various forces reaches a certain threshold. After that, a bondage was formed between the two molecules. Importantly, the antibodies did not distinguish between molecules based on their origin or sequence variance.

The binding affinity of H1-74 was influenced by diverse functional units or combinations of key amino acid residues within its CDR, as shown in Table 2. This variability forms the basis for antibody cross-reaction. The hydrophobic effects were more pronounced between WPFQNY and H1-74 when compared to LPFQNI, which was attributed to the greater binding surface area and the larger W side chain group, in contrast to the small L size. In addition, amino acid I formed a hydrogen bond with W55, while Y formed a more intensive hydrogen bond system with residues N36, Y37, and G38 on H1-74. Stronger hydrophobic interactions were also formed between residues Y37 and Y59 on H1-74 and peptide WPFQNY (Figure 2).

In Table 2, the amino acid residues in bold represent those readily binding to epitopes in the static state of the variable region of the antibody. The italicized residues, such as K70, T109, T35, Y59, T60, G38, and G106, are either hidden within the protein structure or distant from the antigen binding region, and remained unaffected by the static state of the antibody. The antibody and polypeptide, which were mutually induced, initially bound together, leading to the exposure of protein allosteric or groups and their subsequent proximity to each other.[26,32] Y214 was the only amino acid among five of the antigen-binding region E that facilitated binding in the antibody's static state. The remaining residues, S217, R216, H212, and Y155, while "prepared" for binding to the antigen, were not utilized in binding to these three polypeptides, suggesting H1-74's potential to bind to more antigen epitopes.

While molecular simulation techniques have shed light on antibody cross-reaction mechanisms, further experimental verification is essential. To enhance our understanding of H1-74's binding to antigen epitopes and its interaction with polypeptides LP-9, LI-6, and WY-6, we routinely immunized BALB/c mice with these three antigen epitope peptides conjugated to BSA. This process produced polyclonal antibodies and mAbs to study the properties of the antigen epitopes H1-74 bound to three polypeptides. Antigenic epitope peptides LP-9 and LI-6 derived from HA stimulated antibody production against the H1N1 influenza virus in mice. However, the modified antigenic epitope peptide WY-6, through binding to H1-74 mAb, failed to induce antibodies against H1N1 influenza virus, as shown in Table 4, and Supporting Information S1: Tables S2 and S3. This suggests the antigen epitopes bound by H1-74 on LI-6 and WY-6 were distinct.

This study's findings suggest that the CDR region of an antibody molecule plays a crucial role in determining antigen-binding conditions. Alterations in key amino acid residues within the CDR can lead to varied immunodominant group combinations, providing a basis for antibody cross-reactivity. Consistent with crystal structure analyses, these results indicate that mAbs can bind to diverse epitopes through different complementary binding regions, based on ligand localization, contributing to antibody poly specificity.[28] This insight is valuable for understanding autoimmune diseases triggered by microbial infections, aiding in early diagnosis. In addition, the cross-reactivity of antibodies to newly emerging pathogenic microbial variants can also be improved by enhancing the conformational flexibility of the antibody skeleton region, which is crucial for the development of effective universal vaccines,[33] which provides a new idea for our future research.

AUTHOR CONTRIBUTIONS

Chunyan Guo and Jun Hu designed the study. Chunyan Guo and Lijun Shang wrote the manuscript. Qing Feng, Xin Xie, Yan Li, and Hanyu Hu performed the experiments. Senbiao Fang guided computer simulations. All authors read and approved the final manuscript.

ACKNOWLEDGMENTS

The study was financed by the Shaanxi Province Natural Science Basic Research Program (Grant no. 2023-JC-QN-0855), the Key Research and Development Program of Shaanxi (Grant no. 2021ZDLSF01-03), and the Incubation Fund Program of Shaanxi Provincial People's Hospital (Grant no. 2021YJY-27).

CONFLICT OF INTEREST STATEMENT

The authors declare no conflict of interest.

DATA AVAILABILITY STATEMENT

The data that support the findings of this study are available from the corresponding author upon reasonable request.

ORCID

Chunyan Guo http://orcid.org/0000-0001-7188-2256
Lijun Shang http://orcid.org/0000-0001-5925-5903

REFERENCES

1. Robles VM, Dürrenberger M, Heinisch T, et al. Structural, kinetic, and docking studies of artificial imine reductases based on biotin-streptavidin technology: an induced lock-and-key hypothesis. *J Am Chem Soc*. 2014;136:15676-15683.
2. Landsteiner K, van der Scheer J. On cross reactions of immune sera to azoproteins. *J Exp Med*. 1936;63(3):325-339.
3. Mitchell AM, Srikumar T, Silhavy TJ. Cyclic enterobacterial common antigen maintains the outer membrane permeability barrier of *Escherichia coli* in a manner controlled by YhdP. *mBio*. 2018;9(4).
4. Forssman J. (die). herstellung hochwertiger spezifischer schafhämonysine ohne verwendung von schafblut. ein beitrag zur lehre von heterologer antikörpebildung. *Biochem Z*. 1911;37:78-115. (in German)
5. James JA, Kaufman KM, Farris AD, Taylor-Albert E, Lehman TJ, Harley JB. An increased prevalence of Epstein-Barr virus infection in young patients suggests a possible etiology for systemic lupus erythematosus. *J Clin Invest*. 1997;100(12):3019-3026.
6. Lagercrantz R, Hammarström S, Perlmann P, Gustafsson BE. Immunological studies in ulcerative colitis. *J Exp Med*. 1968;128(6):1339-1352.
7. Guilherme L, Cunha-Neto E, Tanaka AC, Dulphy N, Toubert A, Kalil J. Heart-directed autoimmunity: the case of rheumatic fever. *J Autoimmun*. 2001;16:363-367.
8. Levin MC, Lee SM, Kalume F, et al. Autoimmunity due to molecular mimicry as a cause of neurological disease. *Nature Med*. 2002;8(5):509-513.
9. Sun L, Li H, Sun J, et al. Antibodies against H1N1 influenza virus hemagglutinin cross-react with prohibitin. *Biochem Biophys Res Commun*. 2019;513(2):446-451.
10. Guo C, Zhang H, Xie X, et al. H1N1 influenza virus epitopes classified by monoclonal antibodies. *Exp Ther Med*. 2018;16(3):2001-2007.
11. Jick SS, Li L, Falcone GJ, Vassilev ZP, Wallander MA. Epidemiology of multiple sclerosis: results from a large observational study in the UK. *J Neurol*. 2015;262:2033-2041.
12. Guo C, Xie X, Li H, et al. Prediction of common epitopes on hemagglutinin of the influenza A virus (H1 subtype). *Exp Mol Pathol*. 2015;98(1):79-84.
13. Xu W, Han L, Lin Z. Screening of random peptide library of hemagglutinin from pandemic 2009 A (H1N1) influenza virus reveals unexpected antigenically important regions. *PLoS ONE*. 2011;6:e18016.
14. Jiang X, Xu X, Zeng L, et al. A gold-based immunochromatographic strip for the detection of sirolimus in human whole blood. *Analyst (Lond)*. 2022;147:1394-1402.
15. Falklind-Jerkérus S, Felici F, Cavalieri C, et al. Peptides mimicking Vibrio cholerae O139 capsular polysaccharide elicit protective antibody response. *Microb Infect*. 2005;7:1453-1460.
16. Han X, Lin H, Chen X, et al. Amide-containing neoepitopes: the key factor in the preparation of hapten-specific antibodies and a strategy to overcome. *Front Immunol*. 2023;14:1144020.
17. Srinivasappa J, Saegusa J, Prabhakar BS, et al. Molecular mimicry: frequency of reactivity of monoclonal antiviral antibodies with normal tissues. *J Virol*. 1986;57(1):397-401.
18. Uversky VN, Van Regenmortel MHV. Mobility and disorder in antibody and antigen binding sites do not prevent immunochemical recognition. *Crit Rev Biochem Mol Biol*. 2021;56(2):149-156.
19. Camacho C, Coulouris G, Avagyan V, et al. BLAST+: architecture and applications. *BMC Bioinform*. 2009;10:421.
20. Lucchese G, Flöel A. Molecular mimicry between SARS-CoV-2 and respiratory pacemaker neurons. *Autoimmun Rev*. 2020;19:102556.
21. Angileri F, Légaré S, Marino Gammazza A, Conway de Macario E, Macario AJL, Cappello F. Is molecular mimicry the culprit in the autoimmune haemolytic anaemia affecting patients with COVID-19? *Br J Haematol*. 2020;190:e92-e93.

22. Megremis S, Walker TDJ, He X, et al. Antibodies against immunogenic epitopes with high sequence identity to SARS-CoV-2 in patients with autoimmune dermatomyositis. *Ann Rheum Dis*. 2020;79:1383-1386.
23. Yuan M, Wu NC, Zhu X, et al. A highly conserved cryptic epitope in the receptor binding domains of SARS-CoV-2 and SARS-CoV. *Science*. 2020;368:630-633.
24. Grąźlewska W, Holec-Gąsior L. Antibody cross-reactivity in serodiagnosis of lyme disease. *Antibodies*. 2023;12(4):63.
25. Lerner A, Benzvi C, Vojdani A. Cross-reactivity and sequence similarity between microbial transglutaminase and human tissue antigens. *Sci Rep*. 2023;13:17526.
26. Sharma A, Zhang X, Dejnirattisai W, et al. The epitope arrangement on flavivirus particles contributes to Mab C10's extraordinary neutralization breadth across Zika and dengue viruses. *Cell*. 2021;184:6052-6066.
27. Lam K, Tremblay JM, Perry K, Ichtchenko K, Shoemaker CB, Jin R. Probing the structure and function of the protease domain of botulinum neurotoxins using single-domain antibodies. *PLoS Pathog*. 2022;18:e1010169.
28. Sethi DK, Agarwal A, Manivel V, Rao KVS, Salunke DM. Differential epitope positioning within the germline antibody paratope enhances promiscuity in the primary immune response. *Immunity*. 2006;24:429-438.
29. Mariuzza RA. Multiple paths to multispecificity. *Immunity*. 2006;24:359-361.
30. Padlan EA, Abergel C, Tipper JP. Identification of specificity-determining residues in antibodies. *FASEB J*. 1995;9(1):133-139.
31. Islam M, Kehoe HP, Lissoos JB, et al. Chemical diversification of simple synthetic antibodies. *ACS Chem Biol*. 2021;16:344-359.
32. James LC, Roversi P, Tawfik DS. Antibody multispecificity mediated by conformational diversity. *Science*. 2003;299(5611):1362-1367.
33. Saini S, Agarwal M, Pradhan A, et al. Exploring the role of framework mutations in enabling breadth of a cross-reactive antibody (CR3022) against the SARS-CoV-2 RBD and its variants of concern. *J Biomol Struct Dyn*. 2023;41:2341-2354.

SUPPORTING INFORMATION

Additional supporting information can be found online in the Supporting Information section at the end of this article.

How to cite this article: Guo C, Feng Q, Xie X, et al. Cross-reaction mediated by distinct key amino acid combinations in the complementary-determining region (CDR) of a monoclonal antibody. *J Med Virol*. 2024;96:e29430. doi:10.1002/jmv.29430